Crystal field theory and excitation spectra in Fe₂Mo₃O₈

© *M.V. Eremin, K.V. Vasin, A.R. Nurmukhametov*[¶]

Institute of Physics, Kazan Federal University,
420111 Kazan, Russia

[¶] e-mail: srgalex@list.ru

The parameters of even and odd crystal fields acting on iron ions in tetrahedral and octahedral positions of the Fe₂Mo₃O₈ crystal are calculated. The obtained energy level schemes of the lowest multiplets are discussed in the context of the available experimental data. By comparing the calculated intensities of magnetic and electric dipole transitions with experimental data, the parameters of the effective Hamiltonian of the interaction of $3d$ electrons with an electric field are refined. It is found that the main absorption lines at $T < T_N$ in the region of terahertz frequencies are due to excitations of iron ions and are not associated with collective oscillations of magnetic moments. The splitting of absorption lines upon application of an external magnetic field is a consequence of the difference in the orientations of the magnetic sublattices relative to the crystallographic axes.

Keywords: Fe₂Mo₃O₈, multiferroics, crystal field, electric dipole transitions.

Introduction

The first studies of compounds (FeM)Mo₃O₈ (where M= Mg, Zn, Mn, Co, Ni) by Mössbauer spectroscopy methods were carried out back in the 1970s [1]. These compounds are quite complex, but possess interesting physical properties. The Fe²⁺ ions in these crystals occupy tetrahedral and octahedral sites. The exchange interaction between ferrous ions leads to magnetic structures, which can change when an external magnetic field is applied and when ferrous ions are partially replaced by nonmagnetic zinc or magnesium ions. Interest in the compound Fe₂Mo₃O₈ as the simplest model object has increased in recent years due to the discovery of giant magnetoelectric effects [2,3] in it, the origin of which has not yet been clarified. Fe₂Mo₃O₈ is a collinear antiferromagnet with the Neel temperature $T_N = 60$ K. When an external magnetic field is applied, the magnetic structure and electric polarization change [3]. In both tetrahedral and octahedral coordinations of Fe²⁺ ions, the ground state is orbitally degenerate multiplets with a rich fine structure. To clarify it in recent years, the technique of terahertz spectroscopy [4,5] has been actively used. However, the interpretation of experimental data is still difficult.

The purpose of this paper is to involve modern methods of the microscopic crystal field theory for this purpose. The first attempts to determine the parameters of the crystal field from the data of Mössbauer spectroscopy were already made in the paper [1]. Then, for this purpose, the technique of terahertz and infrared spectroscopy began to be involved [1,6]. However, this problem has not yet been solved. In particular, the relationship between the phenomenological sets of crystal field parameters and microscopic models of the sites of ferrous ions in these crystals

has not yet been clarified. As it will be shown in this paper, the parameter sets used in [1,6] require important refinements. In particular, it shall be taken into account that the signs of the parameters of the crystal field of the fourth rank for the tetrahedral and octahedral environment of ferrous ions should not be the same, but different. In addition to the microscopic analysis of the parameters of an even crystal field, we also present the results of calculating the parameters of an odd crystal field, which we then use to construct an effective operator for the interaction of $3d$ electrons with an electric field. The origin of absorption lines in the terahertz area of the spectrum and their behavior upon the appliance of the external mangenic field are analyzed. The results of microscopic calculations are corrected and refined by comparison with the available experimental data.

Model and method for calculating energy schemes of ion levels Fe²⁺

Both sites of ferrous ions (A and B) have trigonal symmetry (Fig. 1). The quantization axis is chosen along the the threefold axis.

Taking into account the trigonal symmetry of the sites of ferrous ions, the calculations of the energy level scheme is carried out by means of diagonalizing the energy operator:

$$H = B_0^{(2)}C_0^{(2)} + B_0^{(4)}C_0^{(4)} + B_{\pm3}^{(4)}C_{\pm3}^{(4)} + \lambda LS + \rho(LS)^2$$
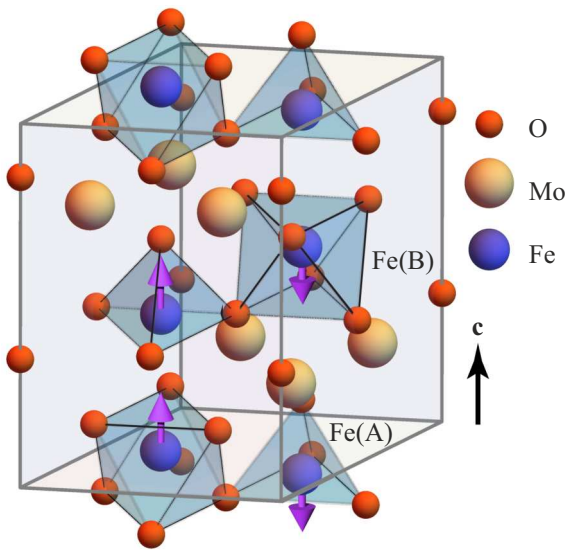$$+ I_z S_z + \mu_B(L_z + 2S_z)B_z. \tag{1}$$

Figure 1. $Fe_2Mo_3O_8$ cell structure [7]. There are two types of sites of Fe^{2+} ions — tetrahedral Fe(A) and octahedral Fe(B) surrounded by oxygen ions. When performing calculations, the z axis is chosen along the c axis, which has hexagonal symmetry (more precisely — this is the direction from the Fe(A) sites to the vertex oxygen atoms). There is a geometrical frustration. „Similar" oxygen coordinations are rotated relative to each other by 180 degrees around the c axis. The arrows show the directions of the magnetic moments of ferrum in the antiferromagnetic phase.

Here $C_q^{(k)}$ — crystal field operators. They are associated with spherical functions by the relation:

$$C_q^{(k)} = \sqrt{\frac{4\pi}{k+1}} \sum_i Y_{k,q}(\theta_i, \phi_i). \qquad (2)$$

The summation in (2) is carried out over all electrons of the $3d$ shell of $Fe^{2+}(3d^6)$. To reduce the number of crystal field parameters, the local coordinate systems were chosen so that the imaginary parts of the crystal field parameters $B_3^{(4)}$ become zero. The letters λ and ρ denote the parameters of the spin-orbit and spin-spin coupling, respectively — their approximate values for Fe^{2+} ions are well known [8].

Calculation method for the intrinsic crystal field parameters

At the first stage of the calculation, the parameters $B_q^{(k)}$ were estimated taking into account the overlapping of wave functions of ferrous ions with the nearest oxygen ions. In the superposition model, i.e. when the system energy is defined as the sum of the energies of individual pairs, the crystal field parameters are determined by the expression at a distance of

$$B_q^{(k)} = \sum a^{(k)}(R_j)(-1)^q C_{-q}^{(k)}(\theta_j, \varphi_j), \qquad (3)$$

where the index j refers to the surrounding lattice ions, $a^{(k)}(R_j)$ — the so-called intrinsic parameters of contributions from lattice ions (ligands) separated from the magnetic ion R_j. In our calculations, the values of $a^{(k)}(R_j)$ contained three terms:

$$a^{(k)}(R_j) = a_{pc}^{(k)}(R_j) + a_{ex}^{(k)}(R_j) + a_{kl}^{(k)}(R_j). \qquad (4)$$

The first term takes into account the electrostatic field from lattice ions with effective charges $Q_j|e|$ and the expression for it is well known [8]. The second term in (4) takes into account the effects of overlapping of the electrons of unfilled shells with the electron shells of the nearest ligands, it was calculated as in exchange charges model [9,10]:

$$a_{ex}^{(k)}(R_j) = G_{ll'} \frac{e^2}{R_j} \frac{(2k+1)}{(l\|C^{(k)}\|l')}$$

$$\times \sum_\rho (-1)^{l-m} \begin{pmatrix} l & k & l' \\ -m & 0 & m' \end{pmatrix} S_{lm,\rho} S_{\rho,l'm'}, \qquad (5)$$

where $G_{ll'}$ — parameters (in the terminology by Malkin — exchange charges on metal-ligand bonds [9]), quantum numbers l, l' refer to the states of unfilled shells of the metal ion, and ρ — to the ligand states. Overlap integrals are calculated (determined) in local coordinate systems with z axes directed along the selected metal-ligand pair G parameter was determined from the splitting of the states of $3d$ electrons by the cubic component of the crystal field.

The third contribution to $a^{(k)}(R_j)$ is due to the electrostatic interaction of $3d$ electrons with the spatially distributed of the ligands electron density of the ligands (oxygen ions). Like the exchange (5), it is mainly due to the nearest oxygen ions. For the first time, Kleiner [11] pointed out the importance of this contribution in the formation of the crystal field, and therefore it is often called the Kleiner contribution. In this paper, this contribution was calculated using the expansion (as in [12]) :

$$U(r) = \frac{Q|e|}{r} + \frac{|e|}{r} \sum_k p_k e^{-\gamma_k r^2}. \qquad (6)$$

Here, the radius r is measured from the ligand core with the effective charge $Q|e|$. The first term in (6) leads to a slight refinement of the contribution from the point charges of the ligands (because it takes into account the integration area $r > R$). The second one — describes the potential energy of $3d$ electrons due to the electrostatic interaction of $3d$ electrons with the spatially distributed density of external ligand electrons (in our case, $2s$- and $2p$ electrons of oxygen). Below this term is denoted by the letter V. The numerical values of p_k and γ_k are given in [12].

Radial wave functions $3d$- and $4p$-electrons were previously written in the form of expansions in Gaussian orbitals:

$$R_{3d}(r) = \sum_i A_i r^2 \exp(-\alpha_i r^2),$$

$$R_{4p}(r) = \sum_j B_j r \exp(-\beta_j r^2). \qquad (7)$$

Table 1. Calculated values of contributions $a_{dd}^{(k)}$ and $a_{pd}^{(k)}$ for tetrahedral and octahedral coordinations of ferrrous ions (in cm^{-1}). R — distance to the contributing ligand (in Å). Exchange contribution is given at $G = 12$. The symbol pc denotes the contribution from point charges, kl — Kleiner and ex — exchange

Contributions	FeO_4				FeO_6			
	pc	kl	ex	R	pc	kl	ex	R
$a_{dd}^{(2)}$	12294	-12571	4312	1.9456	10217	-12571	4312	2.0694
$a_{dd}^{(2)}$	11587	-10696	3535	2.0041	9000	-10696	3535	2.1588
$a_{dd}^{(4)}$	2933	-4448	3607	1.9456	2155	-4448	3607	2.0694
$a_{dd}^{(4)}$	2527	-3653	3040	2.0041	1744	-3653	3040	2.1588
$a_{pd}^{(1)}$	24695	-9705	15357	1.9456	21806	-9705	15357	2.0694
$a_{pd}^{(1)}$	23251	-8577	13627	2.0041	20038	-8577	13627	2.1588
$a_{pd}^{(3)}$	11831	-16218	13911	1.9456	9224	-16218	13911	2.0694
$a_{pd}^{(3)}$	10487	-13787	12488	2.0041	7789	-13787	12488	2.1588

The advantage of using the expansion of the form (7) is due to the fact that the formulas for calculating the contribution from the ligand electron spatial distributions (the Kleiner contribution) can be expressed in closed form. Some of these formulas are given in [13]. When performing this research, the following formulas were additionally required:

$$a_{kl}^{(1)}\left(\frac{1}{r_b}\right) = \frac{3e^2R}{2}\sum_{i,j}\frac{A_iB_j}{\alpha^2}$$
$$\times \int_0^1 \left[\frac{5}{2}y^2(1-y^2) + \alpha R^2y^6\right]\exp(-\alpha R^2y^2)dy,$$

$$a_{kl}^{(3)}\left(\frac{1}{r_b}\right) = \frac{7e^2R^3}{2}\sum_{i,j}\frac{A_iB_j}{\alpha}\int_0^1 y^6\exp(-\alpha R^2y^2)dy,$$

$$a_{kl}^{(1)}(V) = \frac{3e^2R}{4}\sum_{i,j,k}\frac{p_kA_iB_j}{\xi^3}$$
$$\times \int_0^1 z\left(\frac{2R^2}{\xi}z^2 + 5 - 5y^2\right)\exp\left(-\frac{\alpha^2R^2}{\xi}y^2\right)dy, \quad (8)$$

$$a_{kl}^{(3)}(V) = \frac{7e^2R^3}{2}\sum_{i,j,k}\frac{p_kA_iB_j}{\xi^4}\int_0^1 z^3\exp\left(-\frac{\alpha R^2}{\xi}z\right)dy,$$

where e — electron charge and the designations are introduced: $z = (y^2\alpha + \gamma)$, $\xi = \gamma_k + \alpha$, $\alpha = \alpha_i + \beta_j$.

The calculated values of the intrinsic parameters required to calculate the crystal fields from the nearest oxygen ions in octahedral (FeO_6) and tetrahedral (FeO_4) fragments are given in Table 1. Let us note that these parameters are comparable and therefore can be used for other oxides with

Fe^{2+} ions. The radial functions necessary for us were taken from the papers [14,15].

The values of the parameters of the crystal field and the interaction with exchange (molecular) fields obtained by us differ from those encountered earlier. Thus, in the paper [1] the crystal field operator was used in the form

$$H_{cf} = B_2^0O_2^0 + B_4^0O_4^0 + B_4^3O_4^3, \quad (9)$$

where O_n^m — operator equivalents, which were widely used in crystal field theory before the advent of the technique of irreducible tensor operators [8]. The values obtained in [1] were corrected taking into account new experimental data in [6]. Following the modern literature on the theory of crystal fields, we use the crystal field operator in the form:

$$H_{cf} = B_0^{(2)}C_0^{(2)} + B_0^{(4)}C_0^{(4)} + B_3^{(4)}C_3^{(4)} + B_{-3}^{(4)}C_{-3}^{(4)}. \quad (10)$$

As noted in the text, for both sites local coordinate systems can be selected so that the imaginary part of the $B_{\pm3}^{(4)}$ parameters is equal to zero. In this case, the number of parameters in (9) and (10) is the same, and they can be compared. The parameter values recalculated by us from the papers [1,6] are given in Table 2.

The most important difference between our set of parameters and the results of [1,6] is that the signs of $B_0^{(4)}$ for the tetrahedral and octahedral fragments are opposite to each other, not the same. It should be noted that the sign of the real part of $B_3^{(4)}$ changes to the opposite when the coordinate system is rotated by $60°$ or $120°$ around the c crystal axis. Therefore, in the expressions for the energy levels in the absence of a transverse magnetic field, it appears only in absolute value. In this connection, the difference in the sign of the parameter $B_3^{(4)}$ is not critical.

Table 2. Comparison of even crystal field parameters (in cm^{-1}) for Fe$_2$Mo$_3$O$_8$

Parameters		This study	Varret et al. [1]	Stanislavchuk et al. [6]
Fe(A)	$B_0^{(2)}$	1250	158	233
	$B_0^{(4)}$	5500	-5507	-4148
	$B_3^{(4)}$	6040	-6693	-5067
Fe(B)	$B_0^{(2)}$	1020	2772	4172
	$B_0^{(4)}$	-10400	-17570	-16562
	$B_3^{(4)}$	-11500	16733	11462

Calculation of the energy scheme of levels

At the second step of calculations, the Hamiltonian (1) was numerically diagonalized in the basis of all states of the ground terms of ferrous ions ^5D. To estimate the parameters of the molecular fields I_z, the calculation results of the parameters of exchange interactions given in the papers [16,17] were taken into account. Then the parameters of the interactions entering into (1) were corrected according to the available experimental data. For tetrahedral coordination, the ground state of Fe^{2+} is the orbital doublet ^5E, for octahedral it is the orbital triplet $^5T_2$. The energy interval between the ^5E and $^5T_2$ multiplets (terms) according to the spectroscopic data of the paper [18] in site A is 0.5$-$0.6 eV, and in site B — approximately 1.1$-$1.5 eV. The transitions probabilities calculated by us taking into account splittings by the crystal field and spin-orbit interaction for this frequency range are shown in Fig. 2. The magnetic moments of the ground states of ferrous ions measured by the methods of Mössbauer spectroscopy are: $4.21\,\mu_B$ in A-site and $4.83\,\mu_B$ in B-site [1]. The data of terahertz spectroscopy [4], some of which will be given below when comparing the calculation with experiment were taken into account.

It is known that in undistorted tetrahedral and octahedral coordinations $B_0^{(2)} = 0$ and $\mathrm{Re}(B_{\pm3}^{(4)}) = \sqrt{10/7}B_0^{(4)}$. In accordance with the known results [8] for $\lambda = \rho = 0$ we have an orbital triplet and an orbital doublet. The results of calculating the energy levels of the ground multiplets are given in Table 3.

A comparison of the energy levels given in Table 3 shows that in the paramagnetic phase the fine structure of the Fe$^{2+}(^5E)$ multiplet is mainly determined by the low-symmetry crystal field component, while the spin-orbit and spin-spin interactions play a lesser role. The fine structure of the $^5T_2$ multiplet, on the contrary, is mainly formed by the spin-orbit interaction; one can talk about multiplets with fictitious moment $j = 3/2, 5/2$ and $7/2$. The low-symmetry
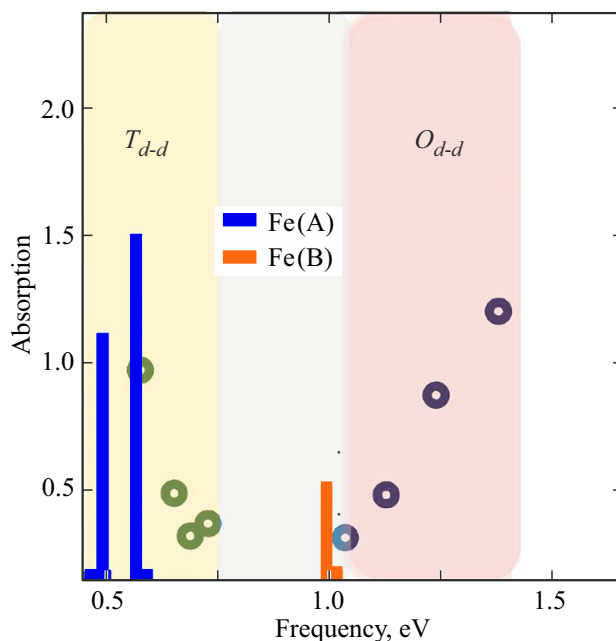

Figure 2. Absorption spectrum of the sample in the IR area. The calculated absorption coefficients are represented by vertical segments, circles — experimental data from the work [18], T_{d-d} and O_{d-d} — designation of the absorption bands belonging to the Fe(A) and Fe(B) sites, respectively.

components of the crystal field play a smaller role for the octahedral site, but they are still quite large and lead to mixing of the states of the $j = 3/2, 5/2$ and $7/2$ multiplets. In the antiferromagnetic phase, an exchange (molecular) field affects the formation of the energy scheme. Its action is equivalent to a strong internal magnetic field. When a relatively weak external magnetic field is switched on, the strengths of the exchange and external fields in one of the spin sublattices are added, while in the other sublattice they are subtracted. As a result, „apparent" splitting of lines of the antiferromagnetic phase into two appear in the excitation spectrum of an antiferromagnet in the general case. Below this effect will be described in more detail when comparing the calculation with experimental data.

Effective operator of interaction with the electric field of a light wave

Since the tetrahedral site of the ion does not have an inversion center, at the beginning of the research it was assumed that the magnetoelectric effects are mainly due to ferrous ions in the A-sites, and ferrous ions in the B-sites play a secondary role. However, the analysis of the structural data obtained in paper [17] and the calculation of odd crystal fields showed that the octahedral site of the ferrous ion also does not have an inversion center, since the crystal structure of Fe$_2$Mo$_3$O$_8$ is rather strongly distorted.

Table 3. Energy levels of Fe^{2+} in tetrahedral and octahedral sites (in cm^{-1}). All parameters of the Hamiltonian are specified in cm^{-1}. For each site, 5 columns are given: the first two refer to the paramagnetic phase ($I_z = 0$), the last three — to the antiferromagnetic (AFM). Column №1 — case of undistorted crystal structure of $\left(B_3^{(4)} = \sqrt{10/7}B_0^{(4)}\right.$ and $\left.B_0^{(2)} = 0\right)$; №2 —distortions of the crystal lattice $\left(B_3^{(4)} \neq \sqrt{10/7}B_0^{(4)}\right.$ and $\left.B_0^{(2)} \neq 0\right)$ are taken into account; №3 — AFM phase in zero magnetic field; №4 and №5 — energies in sublattices of antiferromagnetic phases with spin directed respectively against and along the external magnetic field $B_z = 7\,T$

Tetrahedral site(^5E) $B_0^{(2)} = 1250, B_0^{(4)} = 5500, B_3^{(4)} = 6040$ $\lambda = -70, \rho = 0.2, I_z = 72.5$					Octahedral site($^5T_2$) $B_0^{(2)} = 1020, B_0^{(4)} = -10400, B_3^{(4)} = -11500$ $\lambda = -70, \rho = 0.2, I_z = 72.5$				
№1	№2	№3	№4	№5	№1	№2	№3	№4	№5
					426	508	735	848	795
					426	506	702	792	747
					426	506	679	790	740
					417	495	655	724	689
					417	495	623	663	638
39	51	337	364	309	417	495	576	592	576
21	48	289	318	261	405	410	477	527	483
21	37	253	273	232	167	409	430	481	469
21	37	229	251	207	167	243	309	386	346
14	24	170	185	156	167	243	297	339	301
14	24	170	184	155	162	168	269	322	295
7	16	108	116	100	162	131	260	318	290
7	6	90	97	83	0	34	174	281	228
0	6	42	44	41	0	0	113	154	135
0	0	0	0	0	0	0	0	0	0

The absence of an inversion center at the sites of ferrous ions leads to the appearance of odd crystal fields on them, which induce transitions between the ground configuration $3d^6$ and $3d^54p$, thus allowing electric dipole transitions. The effective interaction operator of $3d$-electrons with an electric field in both sites A and B can be described by the following expression [19]:

$$H_E = \sum_{p,t,k} \left\{E^{(1)}U^{(k)}\right\}_t^{(p)} D_t^{(1k)p}. \qquad (11)$$

Here the curly brackets denote the direct (Kronecker) product of the spherical components of the electric field $E_0^{(1)} = E_z$, $E_{\pm 1}^{(1)} = \mp\left(E_x \pm iE_y\right)/\sqrt{2}$ and the unit tensor operator $U_q^{(k)}$. Summation indices take values $k = 0$, 2, 4, $p = 1$, 3, 5, $t = 0$, ± 3. In coordinate systems with $\mathrm{Im}\left(B_3^{(4)}\right) = 0$, the imaginary parts of the parameters of the effective dipole moment $D_t^{(1k)p}$ with $t = 3$ are also equal to zero.

The parameters $D_t^{(1k)p}$ were calculated on the basis of the Hartree-Fock wave functions of ferrous and oxygen ions in the same way as it was done in [20,21] for ferrous ions in FeV_2O_4 and in $FeCr_2O_4$, and then they were corrected to match the relative intensities of electric and magnetic dipole transitions in terahertz spectra [4]. In order of magnitude and signs, they correspond to those obtained earlier as a result of microscopic calculations and in describing the effect of an optical diode in a $FeZnMo_3O_8$ crystal (sites B) [21].

Let us note that in the superposition model, for the quantities $D_t^{(1k)p}$, a relation similar to (3) holds true:

$$D_t^{(1k)p} = \sum_j d^{(1k)p}\left(R_j\right)\left(-1\right)^t C_{-t}^{(p)}\left(\theta_j, \phi_j\right). \qquad (12)$$

It is a consequence of the assumed axial symmetry in the metal-ligand pair. However, in contrast to the internal parameters of the $a^{(k)}\left(R_j\right)$ crystal field, the $d^{(1k)p}\left(R_j\right)$ values do not have the comparability property. This is due to the fact that the expressions for calculating $d^{(1k)p}\left(R_j\right)$ include the parameters of an odd crystal field, which are determined not only by the nearest ligands, but also by remote ones.

It can be seen from Table 3 that the lowest energy levels change quite strongly during the phase transition due to a change in the exchange (molecular) field (parameter I_z). Accordingly, the wave functions also change, which leads to a change in the matrix elements from the operator of interaction with the electric field. The intensities of the total electric dipole transitions (9), calculated for the parameters from Table 3, and the magnetic dipole transitions are shown in Figs. 2, 3.

Comparison with the results of spectroscopic studies

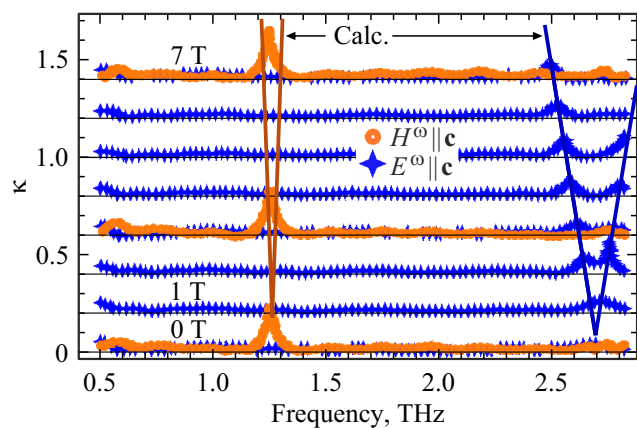As can be seen from Fig. 2 and 3, the calculation results correspond to the spectroscopic data both in terms of the

Figure 3. Calculated terahertz absorption spectra for two polarizations of light in a constant magnetic field along the *c* axis. The magnetic field strength varies from 0 to 7 T. Vertical lines — result of calculation, curves with symbols — experimental data of the paper [4]. When plotting the calculated lines, the real relative absorption intensities are taken into account, and not only the site in the magnetic field (the initial site of the line corresponds to the intensity at 0 T).

site of the absorption lines and their intensities. The values of magnetic moments calculated by us at low temperatures ($4.21\mu_B$ in A-site and $4.83\mu_B$ in B-site) also agree with the data of the paper [1] on the Messbauer spectroscopy study The splitting of the line by 1.25 THz in our calculation is probably somewhat overestimated. In this connection, we note that the magnitudes of the splitting effects were not adjusted in our calculation. When refining the calculation parameters, we focused exclusively on the position of the lines in a zero magnetic field, their intensities, and on the magnitudes of the magnetic moments of ferrous ions at the A and B sites. The novelty of the result obtained here also lies in the fact that we have shown that the main lines in the excitation spectrum in the terahertz area of the antiferromagnet $Fe_2Mo_3O_8$ are due to transitions between the levels of the fine structure of ferrous ions, and not to collective excitations (electromagnons), as it is was assumed in [4]. It is obvious that collective excitations are also present, but the spectral weight of these excitations is less than the total magnetic and induced electric dipole transitions between the components of the fine structure of the lowest multiplets of ferrous ions

Conclusion

The parameters of the even and odd crystal fields acting on ferrous ions in octahedral and tetrahedral sites in $Fe_2Mo_3O_8$ crystal are determined. Their values and signs are consistent with the features of the crystal structure. In particular, it was shown that the signs of the crystal field parameter $B_0^{(4)}$ for octahedral and tetrahedral sites in the $Fe_2Mo_3O_8$ crystal are opposite to each other, as

expected from the experience of studying other compounds activated by transition metal ions. The internal parameters due to the interaction with the nearest oxygen ions are calculated. As part of the superposition model these parameters are comparable and therefore can be used for other oxides with Fe^{2+} An effective operator for the interaction of 3*d* electrons of ferrous ions with an electric field is proposed. It has been tested in calculations of the relative intensities of transitions in the excitation spectra in the terahertz area of the spectrum for various polarizations of the incident electromagnetic wave. It is found that the matrix elements of magnetic and electric dipole transitions in the excitation spectra are comparable in magnitude. The constructed operator of interaction with an electric field can also be used in calculating various magnetoelectric effects, for example, when the electric polarization changes during magnetic phase transitions. The splitting of absorption lines in the antiferromagnetic phase upon application of an external field („Zeeman pseudoeffect") is explained by the different orientation of the magnetic moments of the antiferromagnetic sublattices with respect to the external magnetic field. Among the general conclusions, the following can be noted. We have shown that the main lines in the excitation spectrum in the terahertz area of the antiferromagnet $Fe_2Mo_3O_8$ are due to transitions between the energy levels of ferrous ions, rather than the manifestation of collective excitations, as was originally assumed. This conclusion, in our opinion, applies to a wide class of magnets containing ions in orbitally degenerate states and located in sites without an inversion center. The latter circumstance determines the presence of sufficiently intense induced electric dipole transitions.

Funding

Conflict of interest

The authors declare that they have no conflict of interest.

References

[1] F. Varret, H. Czeskleba, F. Hartmann-Boutron, P. Imbert. J. Phys. France., **33**, 549 (1972). DOI: 10.1051/jphys:01972003305-6054900

[2] T. Kurumaji, S. Ishiwata, Y. Tokura. Phys. Rev., **5**, 031034 (2015). DOI: 10.1103/PhysRevX.5.031034

[3] Yazhong Wang, Gheorghe L. Pascut, Bin Gao, Trevor A. Tyson, Kristjan Haule, Valery Kiryukhin, Sang-Wook Cheong. Sci. Rep., **5**, 12268 (2015). DOI: 10.1038/srep12268

[4] T. Kurumaji, Y. Takahashi, J. Fujioka, R. Masuda, H. Shishikura, S. Ishiwata, Y. Tokura. Phys. Rev. B, **95**, 020405(R) (2017). DOI: 10.1103/PhysRevB.95.020405

[5] B. Csizi, S. Reschke, A. Strinić, L. Prodan, V. Tsurkan, I. Kézsmárki, J. Deisenhofer. Phys. Rev. B, **102**, 174407 (2020). DOI: 10.1103/PhysRevB.102.174407

[6] T.N. Stanislavchuk, G.L. Pascut, A.P. Litvinchuk, Z. Liu, Sungkyun Choi, M.J. Gutmann, B. Gao, K. Haule, V. Kiryukhin, S.-W. Cheong, A.A. Sirenko. Phys. Rev. B, **102**, 115139 (2020). DOI: 10.1103/PhysRevB.102.115139

[7] S. Reschke, A.A. Tsirlin, N. Khan, L. Prodan, V. Tsurkan, I. Kézsmárki, J. Deisenhofer. Phys. Rev. B, **102**, 094307 (2020). DOI: 10.1103/PhysRevB.102.094307

[8] A. Abragam, B. Bleaney. *Electron Paramagnetic Resonance of Transition Ions* (Oxford University Press, Oxford, 2012).

[9] B.Z. Malkin. *Modern Problems in Condensed Matter Sciences*, ed. by Kaplyanskii A.A., Macfarlane R.M. (Elsevier, Amsterdam, 1987), v. 21, chap. 2, p. 13−50.

[10] M.V. Eremin, A.A. Kornienko. Phys. Stat. Sol. B, **79**, 775 (1977).

[11] W.H. Kleiner. J. Chem. Phys., **20**, 1784 (1952).

[12] V.V. Iglamov, M.V. Eremin. Phys. Solid State, **49**, 229−235 (2007).

[13] K.V. Vasin, M.V. Eremin. J. Phys.: Condens. Matter, **33**, 225501 (2021). DOI: 10.1088/1361-648X/abe730

[14] M. Synek, A.E. Rainis, E.A. Peterson. J. Chem. Phys., **46**, 2039 (1967). DOI: doi.org/10.1063/1.1840999

[15] E. Clementi, A.D. McLean. Phys. Rev., **133**, A419 (1964). DOI: 10.1103/PhysRev.133.A419

[16] I.V. Solovyev, S.V. Streltsov. Phys. Rev. Materials, **3**, 114402 (2019). DOI: 10.1103/PhysRevMaterials.3.114402

[17] S.V. Streltsov, D.-J. Huang, I.V. Solovyev, D.I. Khomskii. JETP Lett., **109**, 786−789 (2019). DOI: 10.1134/S0021364019120026

[18] Y.M. Sheu, Y.M. Chang, C.P. Chang, Y.H. Li, K.R. Babu, G.Y. Guo, T. Kurumaji, Y. Tokura. Phys. Rev. X, **9**, 031038 (2019). DOI: 10.1103/PhysRevX.9.031038

[19] M.V. Eremin. JETP, **129** (6), 1084−1092 (2019). DOI: 10.1134/S1063776119110037.

[20] M.V. Eremin. Phys. Rev. B, **100**, 140404(R) (2019). DOI: 10.1103/PhysRevB.100.140404

[21] K.V. Vasin, M.V. Eremin, A.R. Nurmukhametov. Pisma v ZhETF, **115** (7), 420−423 (2022) (in Russian). DOI: 10.31857/S1234567822070035 [K.V. Vasin, M.V. Eremin, A.R. Nurmukhametov. JETP Letters, **115** (7), 380−383 (2022). DOI: 10.1134/S0021364022100307].

Translated by E.Potapova